The Fourth IEEE RAS/EMBS International Conference
on Biomedical Robotics and Biomechatronics
Roma, Italy. June 24-27, 2012

An Adaptive Sensor Foot for a Bipedal and Quadrupedal Robot

Kristin Fondahl*, Daniel Kuehn*, Frank Beinersdorf*, Felix Bernhard†, Felix Grimminger*, Moritz Schilling†, Tobias Stark† and Frank Kirchner*†

***Abstract*— One key benefit of legged robots is their ability to act on the environment by applying forces in a noncontinuous way in innumerous directions and magnitudes within their designed workspace. Most multi-legged robots are equipped with single-point-contact feet for the sake of simplicity in design and control. This paper focuses on a sophisticated lower limb system for a multi-legged robot to demonstrate the advantages of actuated multi-point-contact feet. Indications for these advantages can be found in nature, where the mechanical and sensory interaction of the feet with the substrate enables highly flexible ways of locomotion in animals and helps to optimize traction. Multi-point-contact feet even enable the transition from quadrupedal to bipedal walking, a dexterous behavior of ape-like mammals. To prove the technical plausibility of the planned leg structure, a first prototype including a lower leg, an actuated ankle joint, an attached foot structure, and a set of sensors with their required electronics was developed and integrated. Due to its characteristics, the lower limb – as a subcomponent of a legged robotic system – will extend the robot's knowledge of its internal and the environmental states. The mechanical and electronic design of the foot structure is presented in this paper as the basis for a later development of a biologically inspired control scheme.**

I. INTRODUCTION

More than half a century has passed since the concepts of legged locomotion started to be of increasing interest for researchers dealing with robot mobility as an alternative or in addition to established wheel- and track-based approaches [1, p. 362].

The motivation to concentrate research on this kind of locomotion is due to the possible advantages and versatility of such systems such as: (i) decoupling body orientation from terrain structure, (ii) no need for a continuous ground contact path, (iii) ascent, descent, and traverse of steep slopes, (iv) numerous ways to apply forces to the environment, (v) handling a wide variety of substrates, (vi) use of appendages (legs) as a tool carrier for manipulation tasks, (vii) inherent redundancy and (viii) omnidirectional mobility, among others. These stated advantages come at the expense of the system's mechanical and control simplicity. Nevertheless, by looking at possible fields of application, the benefits of dealing with this extra complexity become clear.

* Kristin Fondahl, Frank Beinersdorf, Felix Grimminger, Daniel Kuehn, and Frank Kirchner are members of the German Research Center for Artificial Intelligence Robotics Innovation Center, 28359 Bremen, Germany.

† Felix Bernhard, Moritz Schilling, Tobias Stark, and Frank Kirchner are members of the University of Bremen, FB3, Robotics Lab, 28359 Bremen, Germany. All authors contributed equally to this work.

Contact: daniel.kuehn@dfki.de

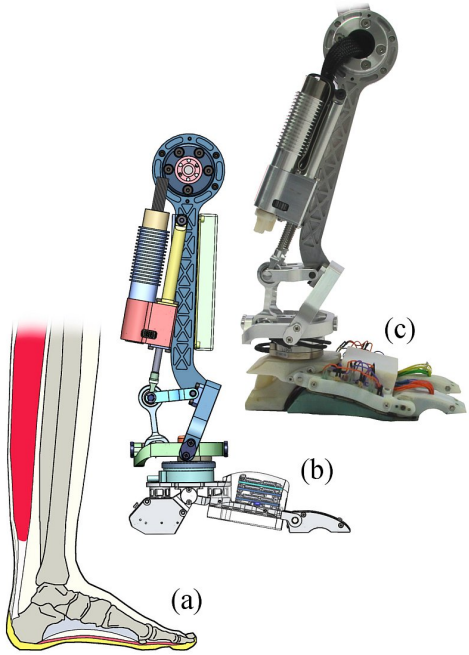

Fig. 1. **Lower leg / ankle joint / foot - assembly**: Next to the biological inspiration (a), the CAD-model (b) depicts the desired lower leg structure. (c) shows a photograph of the lower leg and ankle joint with a preliminary version of the foot made from a Rapid Prototyping material.

Aim of the project *iStruct* is the development of a four-legged robotic research platform with the ability to perform quadrupedal and bipedal locomotion [2]. The basic task is to evaluate the possible transfer of control mechanisms for quadrupedal to bipedal locomotion. How will the pattern and activation musters have to be modified to serve both locomotion modes, or are the control structures purely four- or two-legged-specific? The presented electro-mechanical foot structure (Fig. 1) allows the analysis of these questions. The design offers a challenge in itself: How to build and integrate a foot-like structure which includes the high amount of sensors that is needed to provide the proprio- and exteroceptive information necessary to control the system? Inspiring archetypes for versatile locomotion modes are chimpanzees (*Pan troglodytes*) which frequently switch between bi- and quadrupedal walking. The limb proportions and other features of primate legs and feet useful for walking were analyzed and served as a guideline for the design of the leg structure. As to the foot structure, the focus was widened, due to a lack of documentation for chimpanzee feet, to all

978-1-4577-1200-5/12/$26.00 ©2012 IEEE

primate feet, including the human foot.

As stated above, one key benefit of legged robots is their ability to act on the environment by applying forces in a noncontinuous way in innumerous directions and magnitudes within their designed workspace. This variability is increasing with the system's number of degrees of freedom (DOFs). One key aspect of the project is to go a step further in the complexity of the robot's morphology by introducing an active spine-based torso [2]. These additional DOFs will give rise to an increased overall range of motion, step length, and improved manipulation capabilities.

Another aspect of the project and subject of this paper is the improvement of the robot's capability to handle the interaction forces with the ground. Most bipedal robots have multi-point-contact feet (MPCF) attached to a passively constrained and/or actuated ankle joint to realize a stable stance by spanning a global support polygon ([1, p. 371]).

This function of MPCF is not that important for multi-legged robots which have the intrinsic ability to generate a stable stance by selecting an appropriate ground contact pattern even with single-point-contact feet (SPCF). Consequently, to simplify design and control, the majority of these systems neglect the foot issue (cf. [3], [4], [5], [6]). Still, MPCF can have advantages for multi-legged locomotion as well, such as a better adaptation to difficult terrain which leads to increased traction. The existing multi-legged walking robots that feature MPCF (e.g. [7], [8]), have passive adaptation mechanisms in the feet to exploit these benefits. While this purely passive adaptation is sufficient for effective quadrupedal walking, it hinders a stable and efficient locomotion in bipedal walking. Since the combination of these two locomotion modes is a focus of the project, new active MPCF suitable for both locomotion modes had to be developed.

The project's long-term goal is to demonstrate the advantages of a complex 3-DOF ankle joint with an attached MPCF structure. As a first step in this direction, a laboratory sample of a lower leg was built focusing on the overall mechanical, sensory, and communication concept, while neglecting the actual foot shape. The foot design was developed in a second step, incorporating demands of the mechanical system as well as taking inspiration from nature.

The mechanical design of the single structures (lower leg, ankle joint, foot) and the required constraints (e.g. actuation) are discussed in Sec II. The whole structure has led to an increased set of variables describing the system's kinematics and interaction force states. This resulted in the integration of an adequate set of sensors and their corresponding electronics (system nodes) described in Sec. III. Subsequently, an overview of the currently implemented ankle joint orientation control strategy is given in Sec. IV.

II. MECHANICAL DESIGN AND ACTUATION

The first step of the design process is to identify the requirements for a bi- and quadrupedal walking system. Therefore, the ranges of motion and proportions of the chimpanzee *Pan troglodytes* were taken as a general guideline in the design (cf. Fig. 2). The completed system will measure

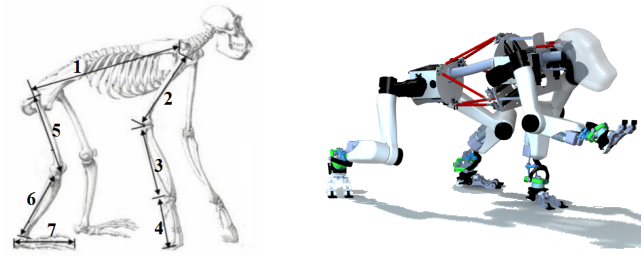

(a) Skeleton of a chimpanzee (adapted from [9])

(b) Design sketch of the planned robot

Fig. 2. Biological archetype (a) and the planned robotic system (b). The proportions of the chimpanzee were used to set the following dimensions for the robot: torso (1) 500 mm, upper and lower arm (2 & 3) each 250 mm, hand (4) 150 mm, upper and lower leg (5 & 6) each 250 mm, foot (7) 200 mm. This led to an approximate system height of 80 cm in a typical quadrupedal pose.

approximately 80 cm in height, at a planned system weight of about 22 kg. A design sketch of the planned ape-like demonstrator is shown in Fig. 2.

The ankle joint's three rotational DOFs are constrained and actuated by two linear actuator units for controlling the foot rotation in the frontal plane (eversion/inversion $\rightarrow$ Roll) and rotation in the sagittal plane (dorsiflexion/plantarflexion $\rightarrow$ Pitch). The remaining rotational DOF in the transverse plane (abduction/aduction $\rightarrow$ Yaw) is constrained by means of a passive, spring-centered limiter.

The developed linear actuators are based on brushless DC motors (BLDC). These motors are supplemented by reduction gear units (10:1) and incremental encoders. The relative position is measured by evaluation of these encoders while digital Hall sensors are used for motor commutation. To reduce the moment of inertia of the whole leg, the ankle drives are located near the knee joint (Fig. 1). For the motor power supply, control, and sensor data acquisition, specifically developed FPGA-based electronics are used.

A lead screw and spindle nut mechanism is connected to the gear's output shaft for the rotational/linear-conversion (lead $=$ 2 mm). To keep the whole unit as short as possible, a parallel arrangement of the motor and the spindle nut rotation axes was chosen. The linear motion is transmitted via two four-bar spatial linkages to the lower ankle joint segment (cf. Fig. 1).

The linkages are used, by simple changes of the lever arm lengths, to adjust the mechanical advantage and the range of motion (ROM) of the foot. According to [10] a ROM in a human foot of roll from 10° to -20°, pitch between 20° to -30°, and yaw from 10° to -10° can be observed. Since apes display a slightly larger range of motion [11], the ROM of the artificial foot is increased; the resulting joint angles for the current configuration are depicted in Fig. 3. Combined with the actuators mentioned above, the maximum angular velocities for the active DOFs of the unloaded ankle joint are 130 °/s for the pitch and 190 °/s for roll motion.

The lower ankle joint segment is an adequate location for measuring the full set of interaction forces and torques induced to the leg. Consequently, a 6-axis Force/Torque

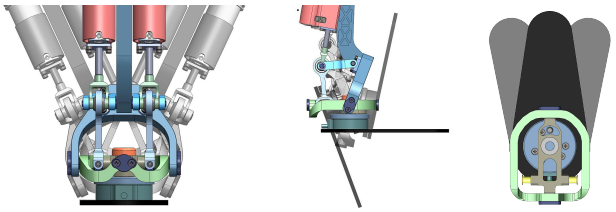

(a) Roll: ±25° (b) Pitch: 130° (c) Yaw: ±20°

Fig. 3. Range of motion of the developed ankle joint

Sensor (F/T-Sensor) is embedded and serves as a well-defined mechanical interface between foot and lower leg.

Due to a better documentation, the foot design is inspired by the human foot. Fig. 4 shows the CAD-model of the foot. It has one DOF of passive compliance in the pitch axis to absorb the first impact of the ground contact and two actuated toes to provide further traction on rough-structured substrates.

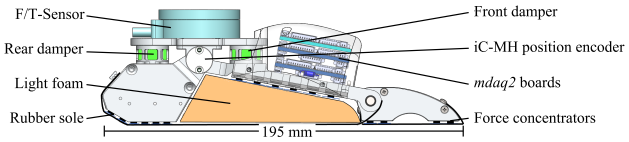

Fig. 4. CAD model of the foot structure at the limit of the damping structures. The IR-sensor and the bowden cables are integrated inside the foot structure and not visible.

Impact damping is realized by the front and rear dampers of the foot arch. The arch also provides a better adaptation to the ground, as the front damper allows the forefoot to passively adjust its orientation. A polymer foam is used as damping material which dissipates energy from the heel-strike and the ball of the foot. When the foot is fully loaded, the two passive dampers run into mechanical limiters to ensure a robust stance and simplify the control of the foot system.

Another characteristic is inspired by the Windlass Mechanism of the human foot (cf. Fig. 5(a), [12]). This mechanism stiffens the human middle foot whenever the toe is dorsiflexed. Looking at this mechanism, a different use of this interconnection was developed. The toes in the artificial foot are actuated via bowden cables which lead from the toes' axes over the back of the foot to an actuator at the lower leg. These cables cannot only be used to actively actuate the toes, they can also serve as a "reverse Windlass effect", when they are led through the sole of the foot. Whenever the robot steps on an obstacle, the sole is pushed inwards. It thus shortens the cables, passively actuating the toes to grip onto the obstacle (cf. Fig. 5(b)).

In order to strive for an equally high sensor density as in primate feet, a pressure sensor array is mechanically embedded in the artificial foot which provides feedback of the distribution of the ground reaction forces. The Force Sensitive Resistors (FSR) have to be shielded from shear stress. Furthermore, they have to be mounted on a plane and no other part than the sensing area may be loaded to avoid the

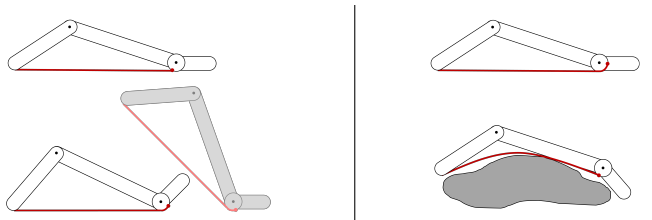

(a) Biological inspiration (b) Technical application

Fig. 5. Function of the biological Windlass effect in the human foot (a) and the "reverse Windlass effect" in the technical application (b).

transmission of an unperceived force onto the foot structure. These requirements resulted in a multi-layer structure of the sole (cf. Fig. 6) which is an adaptation of the concept proposed in [13]. The outermost layer, the actual sole which is in contact with the ground, provides traction as well as mechanical protection of the sensitive inner parts. This layer is to be fabricated from a 1 mm high traction rubber for car tires. The first layer beneath this protection consists of thin metal sheets which are connected by a flexible fabric to avoid shifting. So, the forces are transmitted from a wider area onto rubber cylinders and the flow of force on any other area of the foot is hindered. The rubber cylinders provide the connection between the metal sheets and the sensing area, concentrating the force on the sensing area only. They are guided by a grid to prevent the transmission of shear forces. The sensors in the innermost layer are glued directly into plane prefabricated grooves in the structural components of the foot.

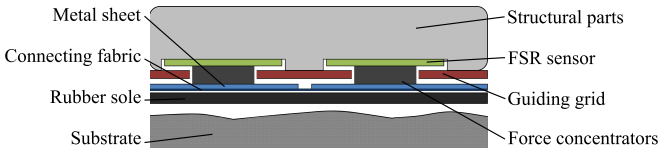

Fig. 6. Schematic overview of the different layers in the pressure-sensing sole of the foot.

III. ELECTRONICS AND SENSORS

A. Electronics

One aspect of the project is the design of compact, generic electronic nodes for each sensory and powered part. A sensor module *mdaq2* (Multiplexed Data AQuisition board) was developed to fulfil these demands with respect to resistive sensors. This module is used to process any resistive sensors used in the current foot design. Fig. 7 gives an overview of this sensor module, and an overview of its major electrical properties is given in Table I.

B. Sensors

The foot is equipped with multiple sensors to account for the additional modes of interaction. A pressure-sensing array was developed to measure the spatial distribution of forces acting on the sole of the foot. This will later enable the robot to adapt to different kinds of ground. In literature, various physical principles (e.g., resistive effect [14], capacitive

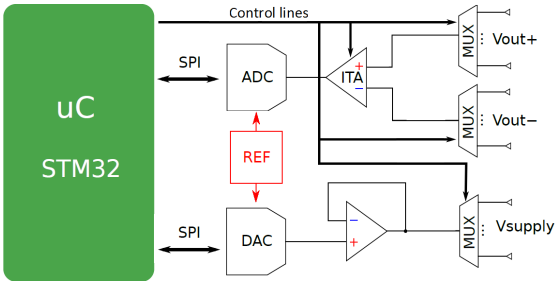

Fig. 7. Schematic overview of the developed resistive sensor module. The module can be used with different types of resistive sensors, e.g. high impedance strain gauges or resistive sensor arrays.

TABLE I

ELECTRICAL PROPERTIES OF THE DEVELOPED *mdaq2*

Analog inputs		
No. Inputs		2×7
Max. input voltage range	$Gain = 1, bipolar$	$\pm 2\,\mathrm{V}$
	$Gain = 1, unipolar$	$0\,\mathrm{V}$ to $4\,\mathrm{V}$
Input impedance	R_{in}	$1 \times 10^9\,\Omega$
Analog outputs		
No. Outputs		7
Output voltage range	V_{out}	$0\,\mathrm{V}$ to $4\,\mathrm{V}$
Max. output current	I_{out}	$250\,\mathrm{mA}$
Dynamic properties		
Settling time	τ_{settle}	$0.780\,\mu\mathrm{s}$ to $1800\,\mu\mathrm{s}$
Power supply		
Main supply voltage	V_{sup}	$5.3\,\mathrm{V}$ to $20\,\mathrm{V}$
Quiescent current	$I_q, V_{sup} = 8\,\mathrm{V}$	$\simeq 64\,\mathrm{mA}$

effect [15], optical effects [16], or mechanical methods [5]) are described to perform this task. The selected kind of sensor is based on the high availability of various resistive sensor types.

The array is made up of 49 FSR which are connected to the *mdaq2* board to determine the conductance of each sensor element. The main load-bearing points on the heel and the toes have a higher sensor density (15 sensors on the heel, 2 x 8 on the toes) than the area inside the foot arch (12 sensors). The six remaining sensors serve as collision detectors on the outside of the foot.

The FSR are sensitive to forces normal to their surface and provide information about the location of these forces. The spatial information is used for the support polygon calculation. Since one aim is also to realize two-legged walking, the support polygon for a single foot is of interest. The force resolution of the array may be insufficient for high loads. Therefore, a F/T-Sensor is mounted at the ankle joint to precisely measure the sum of all forces and torques applied to the foot structure in relation to the leg. The measurements of the F/T-Sensor are captured by a second *mdaq2* board.

The remaining interfaces of the two *mdaq2* boards (e.g. SPI, GPIO) capture the inputs of various other digital sensors. For instance, digital angular encoders are positioned on the axes of the ankle joint and foot to determine the absolute angle of all parts of the foot relative to the lower leg. A digital 3-axis accelerometer will allow the system to sense the gravity field which each foot is exposed to. This field will contain the orientational vector to the center of the earth overlaid by any other accelerations such as those occurring during collision or slip. A distance sensor is mounted on the heel and uses short light impulses to estimate the distance to obstacles. This knowledge offers the opportunity to reduce the force prior to actual ground contact. At last, temperature sensors are embedded in the *mdaq2* boards which allow a temperature compensation of the involved electronic components.

C. Sensory Processing

In order to increase the knowledge of the robot of its own state and that of its environment, the raw sensory data collected on the foot have to be further processed. A first step in this process is the transformation of voltage differences to conductances of the FSR sensor array to measure the actual forces. Following steps will further process this information and combine it with information of the remaining sensors (sensor fusion) to provide abstract system data such as the center of gravity or the support polygon of a foot.

The conductances of a sensor array depend on the pressure which is applied to each sensory element. With the *mdaq2* board, conductances cannot be measured directly because of bypass currents flowing through the resistance network. For each driven row k of the array, all potentials on each row j and column i have to be determined and bypass currents have to be compensated mathematically. As proposed in [17], for each column i Kirchhoff's current law (1) can be used to calculate the conductances of that column.

$$\frac{\vec{V}_i}{R} = M_i \vec{X}_i \tag{1}$$

$\vec{V}_i$ is the potential of each column to ground potential, R is a terminating resistance, and M_i is a matrix consisting of all potential differences between column i and row j. The entries of $\vec{X}_i$ are the conductances in column i. The solutions of the linear systems of equations are the unknown conductances. One way of solving the equations is to invert matrix M_i and calculate $\vec{X}_i$ for each i as suggested in [17]. In lieu of up to seven matrix inversions, the linear systems of equations are solved using Gaussian elimination. Numerical stability is ensured by normalizing each matrix before performing Gaussian elimination with partial pivoting. The acquisition part consists of switching the inputs of the instrumentation amplifier to the analog inputs of interest and the read-out of the sampled values after settling. The influence of noise at small voltage levels is decreased by the repetition of a single measurement at higher gains until either the signal can be clearly distinguished from noise, or the highest possible gain factor (1000) has been reached.

In the default configuration, all matrix elements are measured directly and read-out frequencies of $3.2\,\mathrm{kHz}$/Taxel can be achieved. For an indirect measurement, the update frequency can be increased up to $4.9\,\mathrm{kHz}$/Taxel. Here, the absolute voltages W_j^k and V_i^k are acquired and the entries of M_i are calculated afterwards. Due to the greater time

independence of the measurements, the error caused by noise can be up to $\sqrt{2}$ times as large as with the direct measurement strategy.

The circuitry in [18] uses transimpedance amplifiers on each row and buffers on each column which eliminate the need for bypass current compensation. An update frequency of up to 3 kHz/Taxel was denoted. The approach mentioned in [17] utilizes an amplifier and ADC for each column and row. Here, the update frequency was stated to be up to 1 MHz/Taxel. In comparison, our approach comprises the following advantages. (i) The smaller number of components per taxel leads to a reduced space and current consumption. (ii) The instrumentation amplifier allows signal amplitudes in the order of several µV. (iii) Bypass compensation is performed completely by the onboard microcontroller. (iv) The realized update frequencies are as good as or better than those in [18]. Figure 8 shows a sensor read-out at an update frequency of 3.2 kHz/Taxel. Deviations between each sensory output result from imperfect load distribution, differences between the distinct sensory elements, and cross-talk.

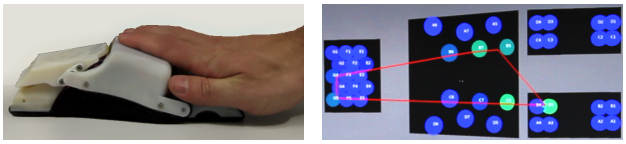

Fig. 8. Example of a sensor array read-out: The RP-model of the foot with the integrated array of FSR-sensors is loaded manually (left) and the results are displayed in the GUI (right).

IV. CONTROL

In order to achieve the stated goals, a distributed control of the robotic system is aspired. As a consequence, the foot should be as self-contained as possible in terms of sensing, sensor preprocessing, and communication to deliver as much information about the surface structure, the condition of the foot, and the interaction between foot and environment. For this, multiple different sensor types and the integration of suitable electronics is necessary. The existing redundancies regarding sensor information within the foot are needed for an evaluation of the sensors, to get additional information about sensor noise, or to be able to exclude permanently incorrect sensory data from the evaluation and thus ensure correct data for the overall system control.

Following the approach of a distributed control system, the low-level control has no information on the context of the processed information. This constraint may be compensated for by using the idea behind predictive control and employing the principle of the efference copy which is known from biological systems. Using internal models on higher level control, the sensor values to expect (sensor blueprint) can be sent to the lowest level. As mentioned before, each sensor is directly connected to a local preprocessing unit. Having a certain computational power in the lowest level, the blueprint can be processed and compared to the actual sensor information.

A precise perception produces a large amount of data. Is the prediction of the incoming data valid and the deviation from the blueprint is smaller than a given error, the raw data itself could be suppressed locally and sent with a minimal frequency to reduce transmission load. This is contemporaneously a keep-alive signal for the high-level control.

An implementation applying low-level local control loops is currently under development. Using the F/T-Sensor, the load applied to the foot while walking is measured. The local control tries to adapt the position of the foot to match the measured forces with the predicted or optimal forces distribution without the necessity to rely on a higher level control. As described above, this behavior is only applied as long as the values of the local control loop are within a certain corridor. If the desired position of the foot deviates too much, the higher level control has to interfere and will take further action to ensure the stability of the system.

Before these approaches for a biologically inspired control scheme can be tested on the robot, the basic control of the system's actuators has to be implemented. The BLDC control electronics and power stage drive the three-phase brushless motors to control the two linear ankle joint actuators.

In Fig. 9, a schematic overview of the FPGA implementation is depicted. To drive the motors according to motion commands (desired pitch and roll; maximal speed), the corresponding motor positions are calculated by an inverse kinematics representation of the ankle joint mechanism in the local FPGA control electronics. Two superposed control loops make up the position control of the motors. The position controller uses the desired position in combination with the sensor feedback to compute the desired speed, while an angle speed controller limits the desired speeds so that both motors finish their motion at the same time to achieve a smooth motion of the ankle joint. The incremental encoder signals are used to calculate the actual speed. In conjunction with the desired speed, this information is used to generate the desired PWM output. The FPGA fullbridge interface currently uses a Hall-sensor based block commutation strategy to switch the gates of the power stage half-bridge MOSFETs. To avoid damage to the hardware, a safety limiter was implemented which monitors the actual joint angles measured by the angular sensors and turns off the motor as soon as the angle's limit is exceeded.

To allow the future integration of impedance control in one of the next motor controller versions, a current measurement was implemented providing the necessary torque estimation of the actuator.

V. CONCLUSION AND FUTURE WORK

This paper presented the mechanical and electronic design of a lower leg, ankle joint, and foot system for a legged robotic research platform that was designed to conduct studies on different control and electro-mechanical aspects of legged locomotion.

The mechanical concept and design of a lower leg assembly which actuates the ankle joint was introduced. Linear actuators were developed using two BLDC motors and a lead

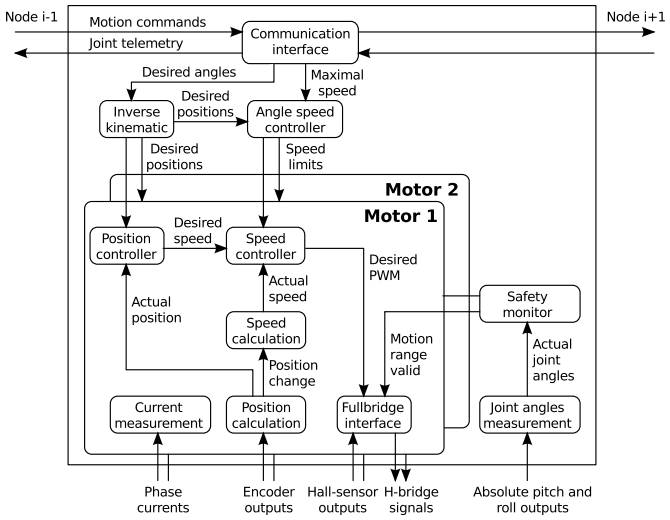

Fig. 9. Schematic overview of the foot actuator control's FPGA implementation in the motor node

screw and spindle nut mechanism. The ankle-joint system was tested successfully, and a control loop was implemented to actuate the ankle joint in its full range of motion and speed.

The biologically inspired mechanical concept of the foot, which was designed to optimize traction, led to a higher need for sensory information. To compensate for this, a pressure sensor array, a 6 DOF-F/T-Sensor in the ankle, and several other sensors that help perceive the state of the robot and its environment were selected and integrated in the foot. The mechanical and electronic sensor integration was tested successfully and the foot was integrated in the software architecture of the research system.

The low-level electronic system is currently capable of determining the conductances of all 49 elements of the sensor array with up to $4.9\,\mathrm{kHz}$/Taxel. It is also able to handle the 6 DOF-F/T-sensor. Work in progress is the calibration of the highly non-linear FSR sensor output to derive pressure densities from conductance densities. This low-level preprocessing allows advanced approaches for the control of the robotic system applying biological principles and predictive control.

The advantages of MPCF, which are a necessity in bipedal locomotion for static balance, will be evaluated for quadrupedal walking. They enable the application of forces in even more directions through the additional active 4-DOFs of the foot. These forces can be precisely controlled due to the abundant sensory information available in the foot structure. The MPCF should thus simplify locomotion on rough terrain. By adapting to the substrate, the ground reaction force can be applied to a wider support area and increase friction even on difficult ground. Furthermore, the high sensor density on the foot may even allow a rough analysis of the ground substrate to adopt a suitable walking behaviour.

VI. ACKNOWLEDGMENTS

We would like to thank all members in our lab who supported us in this work. We would also like to thank Continental for supplying the sole material. This work was performed within the Intelligent Structures for Mobile Robots (*iStruct*) project. The project is funded by the Space Agency of the German Aerospace Center with federal funds of the Federal Ministry of Economics and Technology (BMWi) in accordance with the parliamentary resolution of the German Parliament, grant no. 50RA1013 and grant no. 50RA1014.

REFERENCES

[1] S. Kajita and B. Espiau, "Legged Robots," in *Handbook of Robotics*, B. Siciliano and O. Khatib, Eds. Springer, 2008.

[2] D. Kuehn, F. Grimminger, F. Beinersdorf, F. Bernhard, A. Burchardt, M. Schilling, M. Simnofske, T. Stark, M. Zenzes, and F. Kirchner, "Additional DOFs and Sensors for Bio-inspired Locomotion: Towards Active Spine, Ankle Joints, and Feet for a Quadruped Robot," in *Proceedings of IEEE International Conference on Robotics and Biomimetics. IEEE International Conference on Robotics and Biomimetics (ROBIO), December 7-11, Phuket, Thailand*, 12 2011.

[3] M. P. Murphy, A. Saunders, C. Moreira, A. A. Rizzi, and M. Raibert, "The littledog robot," *The International Journal of Robotics Research*, vol. 30, no. 2, pp. 145–149, 2011.

[4] M. Raibert, K. Blankespoor, G. Nelson, R. Playter, and the BigDog Team, "Bigdog, the rough-terrain quadruped robot," in *Proceedings of the 17th World Congress The International Federation of Automatic Control Seoul, Korea, July 6-11, 2008*, 2008.

[5] S. Bartsch, T. Birnschein, F. Cordes, D. Kuehn, P. Kampmann, J. Hilljegerdes, S. Planthaber, M. Roemmermann, and F. Kirchner, "SpaceClimber: Developement of a six-legged climbing robot for space exploration," in *Proceedings of the International Symposium on Robotics (ISR-2010)*. VDE Verlag GmbH, 2010.

[6] D. Spenneberg and F. Kirchner, "Scorpion: A biomimetic walking robot," in *Robotik 2002, VDI-Bericht*, vol. 1679, 2002, pp. 677–682.

[7] S. Hirose, K. Yoneda, and H. Tsukagoshi, "Titan vii: Quadruped walking and manipulating robot on a steep slope," in *Proceedings of the 1997 IEEE International Conference on Robotics and Automation, Albuquerque, New Mexico*, 1997.

[8] Y. Hong, S. Yi, S. Ryu, and C. Lee, "Design and experimental test of a new robot foot for a quadrupedal joint-leg type robot," in *IEEE International Workshop on Robot and Human Communication*, 1996.

[9] G. Bourne, *The chimpanzee. Anatomy, behaviour, and diseases of chimpanzees*. New York: Karger Basel, 1969.

[10] T. L. Allinger and J. R. Engsberg, "A method to determine the range of motion of the ankle joint complex, in vivo," *Journal of Biomechanics*, vol. 26, no. 1, pp. 69 – 76, 1993.

[11] J. M. DeSilva, "Functional morphology of the ankle and the likelihood of climbing in early hominins," *Proceedings of the National Academy of Sciences*, vol. 106, no. 16, pp. 6567–6572, 2009.

[12] J. Hicks, "The mechanics of the foot - ii. the plantar aponeurosis and the arch," *Journal of Anatomy*, vol. v.88(Pt 1), pp. 345–357, 1954.

[13] C. Doggen, "Foot sensor for 3tu humanoid," 2009, individual Design Assignment University of Twente.

[14] A. Kalamdani, C. Messom, and M. Siegel, "Robots with sensitive feet," *IEEE Instrumentation & Measurement Magazine*, vol. 10, pp. 46–53, 2007.

[15] J. Ulmen and M. Cutkosky, "A robust, low-cost and low-noise artificial skin for human-friendly robots," in *Proceedings of the IEEE International Conference on Robotics and Automation (ICRA)*, 2010.

[16] P. Kampmann and F. Kirchner, "Towards a fine-manipulation system with tactile feedback for deep-sea environments," *Robotics and Autonomous Systems*, 2012, To appear.

[17] Y. Takahashi, K. Nishiwaki, S. Kagami, H. Mizoguchi, and H. Inoue, "High-speed pressure sensor grid for humanoid robot foot," in *IEEE/RSJ International Conference on Intelligent Robots and Systems (IROS)*, aug. 2005, pp. 3909 – 3914.

[18] Y. Yang, M. Cheng, S. S.C., X. Huang, C. Tsao, F. Chang, and F. K.C., "A 32x32 temperature and tactile sensing array using pi-copper films," *International Journal of Advanced Manufacturing Technology*, vol. 46, pp. 945–956, 2010.